Optimizing Bus Stop Environments: Analysis of Sun Glare Reduction with Green Elements in MLS and GPR Data

Silvia. M. González-Collazo [1], Mercedes Solla [1], Elena González [1], Juan L. Rodríguez-Somoza [1], Jesús Balado[1]

[1] Universidade de Vigo, CINTECX, GeoTECH Group. 36310 Vigo, Spain
(silvgonzalez, merchisolla, elena, jlsomoza, jbalado)@uvigo.es

Keywords: Mobile Mapping Systems, LiDAR, Object Classification, Green Infrastructure, Sun Glare, Citizen's Mobility.

Abstract

Urban transportation is pivotal in facilitating citizen mobility, and within this sphere, the thermal comfort experienced at bus stops significantly impacts pedestrians' well-being. This research delves into the analysis of direct sun glare at bus stops utilizing Mobile Laser Scanning (MLS) point clouds. Solar angles are calculated to evaluate sun rays, focusing particularly on the summer solstice, and considering the integration of trees to alleviate direct sun glare. The methodological approach comprises four stages: 1) Semantic segmentation of the bus stop environment, 2) Sun glare analysis, 3) Sun glare analysis integrating trees, and 4) Subsoil investigation with Ground-Penetrating Radar (GPR). Various algorithms, including DBSCAN and filters for height, width, and intensity, are employed to classify different elements contained in the bus stop. Sun rays are then derived based on sun angles, identifying intersections with street elements and vertical structures like bus stops or facades. Subsequently, these intersections are recalculated, incorporating trees in the bus stop vicinity. Finally, GPR is utilized to assess the viability of adding trees. Three bus stops in Vigo, Spain, serve as the focal points of analysis. The study delineates specific time intervals when sun rays either encounter new vegetation obstacles or remain unobstructed. While both small and large trees show potential in reducing sun glare, larger trees notably exhibit greater effectiveness in blocking sun glare for extended periods.

1. Introduction

Elevated air temperatures significantly impact in human thermal comfort and public health, especially in urban areas (Jamei et al., 2016). Exposure to high ambient temperature can increase mortality (Ebi et al., 2021), becoming a public health concern. Heat-related mortality was quantified in (Ballester et al., 2023) during the summer of 2022. They analysed the Eurostat mortality database, estimating 61,672 heat-related deaths in Europe between 30 May and 4 September 2022. Italy (18,010 deaths), Spain (11,324) and Germany (8,173) had the highest summer heat-related mortality numbers, while Italy (295 deaths per million), Greece (280), Spain (237) and Portugal (211) had the highest heat-related mortality rates. Thermal comfort of pedestrians was studied in (Speak & Salbitano, 2022), analysing different urban configurations. Pedestrian path choices were analysed in (Melnikov et al., 2022) considering the sun exposure. In the review made by (Nasrollahi et al., 2020) the authors indicated that the best heat-mitigation strategy for improving thermal comfort was found in vegetation and, specifically, trees because of their shading effect.

The use of bus stops by citizens is linked to sunlight conditions, especially in summer. Some authors studied the bus arrival time prediction (B. Yu et al., 2011), while others analysed routes optimization (Ibeas et al., 2010; Schittekat et al., 2013). However, their primary focus is on waiting times rather than on thermal comfort or solar incidence at bus stops.

Trees are considered as a strategy to enhance thermal comfort in outdoor environments (Coutts et al., 2016; Vailshery et al., 2013). Several studies analysed the incorporation of trees in urban environment to generally improve thermal-comfort conditions (Tan et al., 2017; Tong et al., 2017). Ruiz et al., (2017) compared 12 different urban streets in Mendoza (Argentina) considering tree distribution and thermal comfort. They concluded that there was a 60% improvement in thermal comfort in streets with trees compared to bare ones. Furthermore, in (Kong et al., 2017) tree morphology was examined to analyse how different tree types influence outdoor thermal conditions. They concluded that trees with larger crowns, short trunk, and dense canopy are the most efficient in reducing mean radiant temperature.

To identify urban elements, numerous authors used Mobile Laser Scanning (MLS) point clouds as input data (Teo & Chiu, 2015; Yan et al., 2016). This data type allows obtaining 3D georeferenced information on urban environments and extracting geometric features. Previous studies are mainly based on the characterization of traffic signs, or pole-like elements like traffic lights or trees. Soilán et al., (2016) proposed a method to identify both geometric and semantic properties of traffic signs in urban and highway environments based on MLS point cloud data and RGB imagery. Traffic signs in (Balado et al., 2020) were mapped using data obtained through the Mobile Mapping System (MMS), which included both images and point clouds. Image data was employed for detection and classification, while point clouds were utilized for geo-referencing. The results showed a high level of accuracy, with 89.7% of signals correctly detected, 92.5% accurately classified, and 97.5% precisely located. Yu et al., (2015) studied the extraction of street light poles from MLS point cloud data. Cabo et al., (2014) and Ordóñez et al., (2017) used a voxelization of the MLS point cloud to characterize the pole-like street furniture, and Wu et al., (2013) also applied a voxelization to identify urban vegetation and street trees.

The objective of this study is to develop a method for analysing the effects of sun glare on bus stops and to investigate its mitigation using a solution based on the addition of trees. The proposed method consists of four phases. Initially, a region of interest (ROI) is selected considering the location of the bus stop. The elements within the ROI are classified, focusing on facades, street objects and street furniture that signal to passengers where

This contribution has been peer-reviewed. The double-blind peer-review was conducted on the basis of the full paper.
https://doi.org/10.5194/isprs-annals-X-4-W5-2024-187-2024

to wait or board the bus (vertical bus stops and marquees). Subsequently, calculations are performed to determine the intersections of sun rays with the surrounding elements, considering the actual bus stop. A second analysis is perform considering the addition of trees of different sizes adjacent to the bus stop. Additionally, a Ground-Penetrating Radar (GPR) survey is carried out with the aim of exploring the subsoil and assess the feasibility of planting trees. While MLS informs about the best tree locations, GPR allows reconstructing the subsoil space (Lombardi et al., 2022; Solla et al., 2021), such as the presence of pipes and cables that may compromise tree placement.

This paper is organized as follows. Section 2 presents the proposed method. The results are shown and analysed in Section 3. Finally, Section 4 concludes this work.

2. Method

The proposed method is based on four main steps. Initially, the bus stop is identified, followed by the semantic segmentation of the surrounding bus environment. Then, the incidence of the direct sun glare is analysed, and intersections are calculated. A study is conducted on the solar incidence by adding trees in the immediate vicinity of the bus stop to occlude the direct sun glare. Finally, a subsoil investigation is carried out using a Ground-Penetrating Radar (GPR). Figure 1 shows the workflow of the proposed method.

2.1 Semantic segmentation of bus stop environment

In accordance with the methodology outlined in (González-Collazo et al., 2022), bus stop locations were searched within the MLS point clouds. The bus stop locations are extracted from OpenStreetMaps. Using this data, the nearest point to the bus stop location in the point cloud is selected. Starting from this point, a 30-metre radius search is conducted to define the Region of Interest (ROI). This radius is selected to include all data related to the bus stops, as well as facades, trees, or street furniture that may occlude the sun's rays. Subsequently, a point density reduction is applied to reduce the computational time of further processes.

The semantic segmentation of the ROI elements is executed in two stages. Initially, the points within the ROI are categorised as vertical (points whose main direction is perpendicular to the horizon, such as facades or traffic signs), horizontal (points whose main direction is parallel to the horizon, such as sidewalks or roofs), inclined (points belonging mainly to ramps) and noise points (points captured because of reflections). To accomplish this, tilt $I(Ix, Iy)$ and curvature C are computed from the normals of each point with respect to its k nearest neighbors. The ground inclination Ig is also derived based on trajectory vectors. The curvature threshold is established within the range of $[5, 20]$, while the inclination threshold is defined at a value of 0.03.

Then, a second classification is done to identify the objects inside horizontal, inclined, and vertical elements. Vertical bus stops are searched within vertical elements. This classification is done by applying rasterization ($grid = 0.1\,m$) to the point cloud containing the vertical elements. Based on the obtained raster and the heights, vertical elements are classified into facades, steps, and elements different from steps. The height variance and the difference between the pixel height Hp and the ground height Hg are analyzed in each pixel. Pixels are classified as steps if the height variance is within a threshold of $[0.015\,m, 0.2\,m]$ and the difference between Hp and Hg is less than $0.3\,m$. If the difference between Hp and Hg is higher than $6\,m$, pixels are classified as facades.

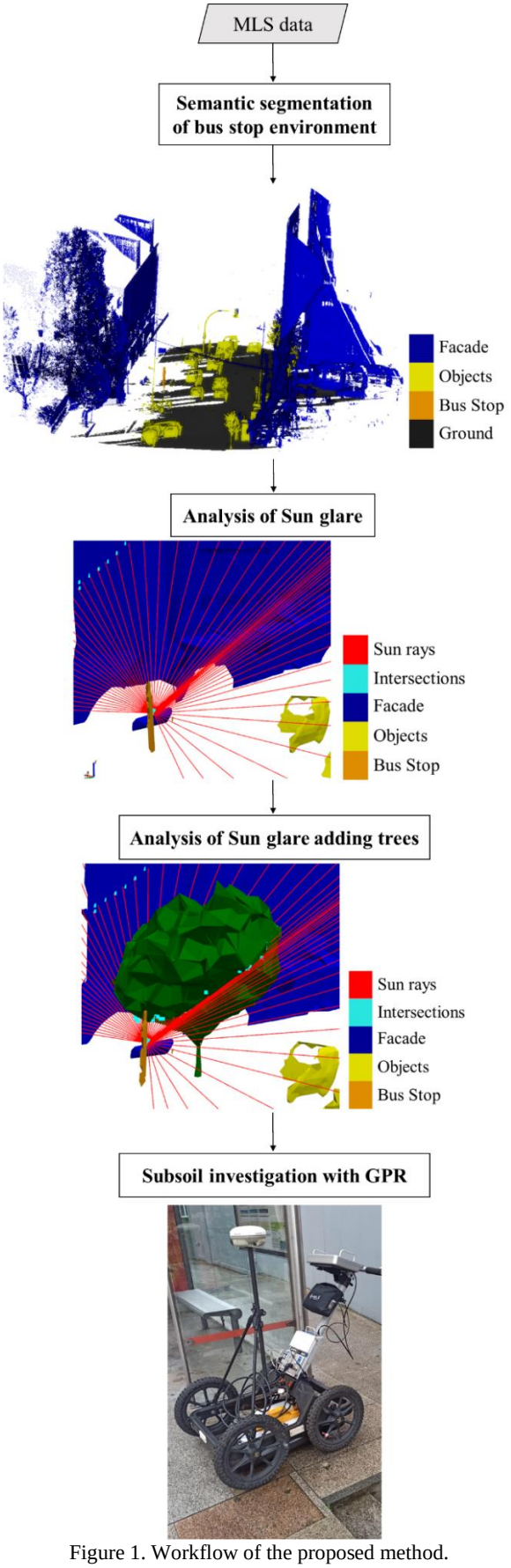

Figure 1. Workflow of the proposed method.

Otherwise, pixels are classified as elements different from steps. This last group is categorized using the DBSCAN algorithm (Wang et al., 2019), which groups the points in clusters based on a minimum distance eps and a minimum number of neighbours $NNmin$. The parameters used in the DBSCAN algorithm to group the points of the horizontal elements in clusters are $eps = 0.1\,m$ and $NNmin = 10$. In this stage, only the vertical elements located in the same space as the sidewalk (regarding the side of the bus stop) are considered. The obtained clusters are classified depending on their height Hc, width Wc, and intensity Ic. If the intensity of the cluster is not higher than the specific value ($Ic < 1000$), the clusters are classified into vertical bus stop depending on their height ($2 \leq Hc \leq 3.2\,m$) and width ($Wc < 0.3\,m$).

Horizontal elements are classified into ground and others. DBSCAN algorithm is used to classify the points into these three groups, using the parameters $eps = 0.1\,m$ and $NNmin = 10$. To classify clusters on ground and other horizontal elements, the height Hc of the cluster is considered. Clusters are classified as ground if Hc is smaller than the ground height Hg plus a height threshold Ht (equal to $0.3\,m$). Clusters that do not fulfill the parameters to be ground are classified as other horizontal elements. Finally, inclined elements are classified into ramps or no ramps using the DBSCAN algorithm, ($eps = 0.1\,m$ and $NNmin = 10$).

To simplify the computation time of the data, the ground was removed. The total ground was obtained merging the steps obtain in the vertical elements, the ramps obtained in the inclined elements and the ground obtained in the horizontal elements.

2.2 Analysis of Sun glare

Sun glare can be an inconvenience for individuals utilizing the bus stop. Therefore, in this stage an examination is conducted on how sun rays affect the bus stop vicinity. The bus stop serves as the reference point for sunray incidence since it is where pedestrians are positioned. Initially, sun rays are calculated based on the solar angles (azimuth β and solar altitude α). Subsequently, intersections of sun rays with obstacles are calculated.

The Sun position is determined for a set of angles measured in degrees, (Figure 2). The declination angle δ (Equation 1) is defined as the angle formed between the ecliptic plane and the equatorial plane. The hour angle ω (Equation 2) represents the angular displacement of the Sun. The solar altitude α is defined as the elevation of the Sun with respect to the horizon. The solar altitude α is represented with Equation 3, where γ is the latitude of the location. The azimuth angle β (Equation 4) is the angle formed by the south direction with the horizontal projection of the straight line connecting the position of the Sun with the observation point.

Angles between south and northeast are negative and angles between south and northwest are positive. Sun rays were calculated each 15 minutes. There is a difference between the solar hour and the clock time. The correction of this difference is defined by (Equation 5), where Lst is the longitude of the country's referenced meridian, C denotes the light saving time correction and ET is a correction factor.

The location of the bus stop is defined as $L = (Lx, Ly, Lz) \rightarrow Nx3$, where N is the number of points. Considering the mean pedestrian's high, Lz is assumed to be the altitude of the road plus 1.7 meters. Therefore, sun rays are defined as $\theta = (Lx, Ly, Lz, \alpha, \beta)$. Intersections of sun rays with obstacles are calculated utilising ROI containing the facade points, street object points and bus stops.

$$\delta = 23.45 sin\left(360 * \frac{284 + N}{365}\right) \quad (1)$$

$$\omega = 15 * (solar\_hour - 12) \quad (2)$$

$$\alpha = asin(sin(\delta) * sin(\gamma) + cos(\delta) * cos(\gamma) * cos(\omega)) \quad (3)$$

$$\beta = asin(cos(\delta) * sin(\omega)/cos(\alpha)) \quad (4)$$

$$Solar\_hour = clock\_time + ET \pm 4(Lst - Lloc) + C \quad (5)$$

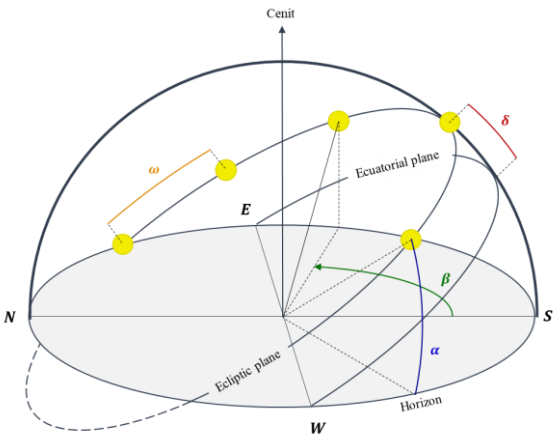

Figure 2. Solar angles

2.3 Analysis of Sun glare adding trees

Following the initial intersection analysis, tree point clouds are automatically incorporated into the original point cloud to evaluate their potential for obstructing solar glare. Trees are positioned exclusively alongside the bus stop, ensuring they do not impede pedestrians or traffic flow. These tests are performed with two size type of trees (Figure 3), which are obtained from an MLS point cloud. A seven meters tree (7mT) consisting of 121,000 points and a four meters tree (4mT) comprising 7,000 points. The 7mT is placed at 2.5 meters from the bus stop (Figure 4), on the side exposed to the incidence of sun rays and the 4mT is placed at 2 meters from the bus stop. With the new point cloud, intersections of sun rays are re-calculated, obtaining new collisions.

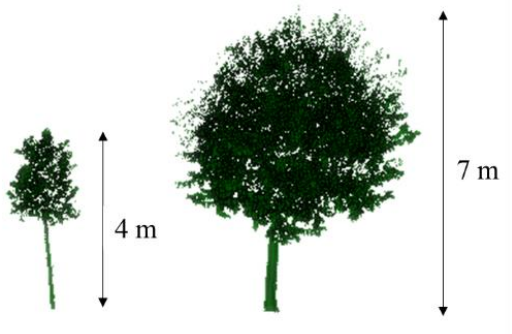

Figure 3. Point cloud of trees

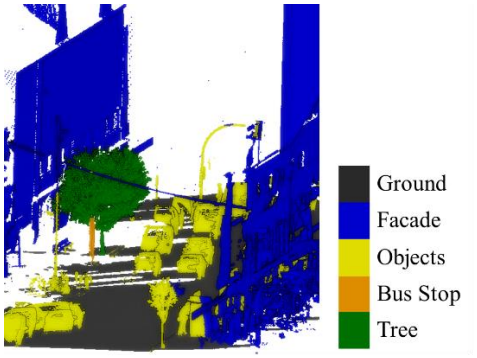

Figure 4. ROI with large tree

3. Experiments and results

3.1 Data

The proposed method was tested in three bus stops in different streets located in Vigo (Spain). Bus stop A and C are located in Castrelos street, and bus stop B is located in Florida street. Figure 5 shows a bus stop example. The input data consisted of urban MLS point clouds, each containing 140 million points, acquired using the Optech LYNX Mobile Mapper. The equipment's specifications are detailed in Table 1.

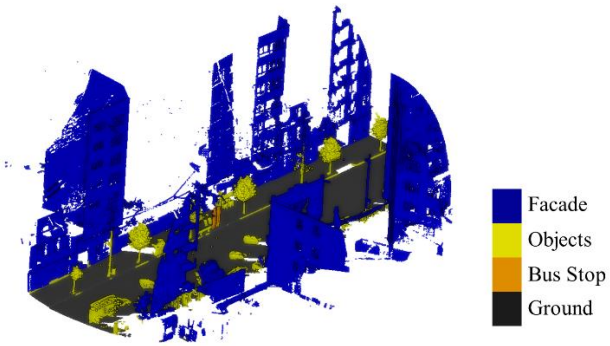

Figure 5. Bus stop (A) MLS point cloud sited in Castrelos street, Vigo (Spain)

LYNX Mobile Mapper OPTECH	
Range (m)	200
Field of view	360° full circle
Precision (mm)	8,1σ
PRF (pulse repetition frequency) (kHz)	75-500
Scan frequency (Hz)	80-200

Table 1. Technical specifications of LYNX Mobile Mapper OPTECH

3.2 Results of Sun glare occlusion with trees

Sun glare was analyzed during the summer solstice (21st June), as this season is distinguished by an augmented solar intensity and an elongated period of daylight. First the analysis was done considering the real conditions of the bus stops and its surroundings. Then, intersections were analyzed adding a tree. Figure 6 shows the results obtained in each bus stop. In this figure are represented the times where there is sun glare and when there are intersections with the built environment (facades, street furniture), with 4mT or with 7mT. During the times where the sun intersects with trees there are no street furniture or facades which occlude the Sun.

Bus stop A		
Solar Hour	Time	Inter.
4:30-4:45	15'	
4:45-5:30	**45'**	
5:30-5:45	15'	
5:45-6:45	**1h**	
6:45-8:45	2h	
8:45-9:00	15'	
9:00-11:45	**2h 45'**	
11:45-12:15	**30'**	
12:15-12:30	15'	
12:30-12:45	15'	
12:45-13:00	15'	
13:00-14:15	**1h 15'**	
14:15-15:30	**1h 15'**	
15:30-18:15	2h 45'	
18:15-19:00	**45'**	
19:00-19:30	30'	

Bus stop B		
Solar Hour	Time	Inter.
4:30-9:00	4h 30'	
9:00-9:45	**45'**	
9:45-10:00	15'	
10:00-10:30	**30'**	
10:30-15:15	4h 45'	
15:15-17:00	**1h 45'**	
17:00-17:45	**45'**	
17:45-18:15	30'	
18:15-19:30	**1h 15'**	

Bus stop C		
Solar Hour	Time	Inter.
4:30-4:45	**15'**	
4:45-5:00	15'	
5:00-5:30	**30'**	
5:30-6:45	1h 15'	
6:45-8:45	**2h**	
8:45-9:45	1h	
9:45-11:30	1h 45'	
11:30-11:45	**15'**	
11:45-12:30	**45'**	
12:30-13:15	**45'**	
13:15-14:15	1h	
14:15-16:15	**2h**	
16:15-19:30	3h 15'	

Sun glare
Intersection with built environment
Intersection with 7mT
Intersection with 4mT or 7mT

Figure 6. Sun glare and Sun ray intersections in bus stops A, B and C

In relation to the findings concerning bus stop A, it can be observed that direct sunlight falls onto the bus stop area during the time intervals from 4:45 to 5:30, 5:45 to 6:45, 14:15 to 15:30, and 18:15 to 19:00. No street obstacles or facades obstruct the sunlight, thus mitigating the occurrence of sun glare. During the time spans from 9:00 to 12:15 and from 13:00 to 14:15, there are no intersections with obstacles or facades that impede the passage of sunlight. Expanding the analysis to incorporate the introduction of trees brings some changes in results, Figure 7. Adjacent to bus stop A, a tree is situated. Nevertheless, the distance between this tree and the bus stop is insufficient to occlude the sun during the time frame from 11:45 to 12:15. On the contrary, when a 4mT is positioned at 2 meters, it successfully obstructs the sun glare. This outcome poses the significance of the tree's placement. If a 7mT is positioned adjacent to the vertical bus stop, the sun is occluded during the periods of time from 9:00 to 12:15 and from 13:00 to 14:15.

In bus stop B there exists a tree besides the bus stop which stands at a height of 5.5 meters. However, in some instances, trees near bus stops may not possess adequate height to occlude the sun during certain hours. In this case, the tree height is not enough to occlude the sun glare during the period from 15:15 to 17:00. Nevertheless, a 7mT effectively mitigates sun glare, Figure 8. In this case, the tree can be allowed to grow until it reaches to attain a height of 7 meters, at which point it occlude the sun glare between 15:15 and 17:00.

For bus stops C, Figure 9, solar glare occurs during the following temporal intervals: from 4:30 to 4:45, from 5:00 to 5:30, from 6:45 to 8:45, from 11:30 to 13:15, and from 14:15 to 16:15. No trees are present in the vicinity of this bus stop. After conducting the analysis with the incorporation of trees, results show that during the interval from 11:30 to 13:15, the trees occlude the sun. In almost all this period, a 7mT is required to effectively occlude the sun's rays. Only during the span from 11:45 to 12:30 is a 4mT adequate.

Solar exposure at bus stops is significantly reduced by adding trees in the vicinity of the bus stop. Especially by adding 7mT. Figure 10 shows the solar exposure time of actual bus stops and the solar exposure time adding trees, both 7mT and 4mT. The outcomes of the intersection analysis after the introduction of a tree pose that these green elements can occlude direct sun glare. While both 4mT and 7mT are capable of mitigating sun glare, it is noteworthy that 7mT tend to effectively block sun glare for longer periods, Table 2. The average of the time reduction adding a 7mT is 3h while adding a 4mT is 37.5'.

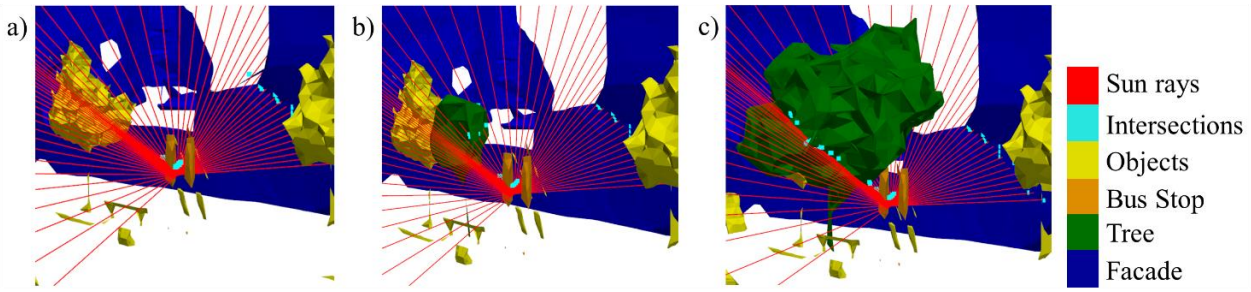

Figure 7. Intersections in bus stop A. a) Real bus stop, b) adding a small tree, c) adding a big tree

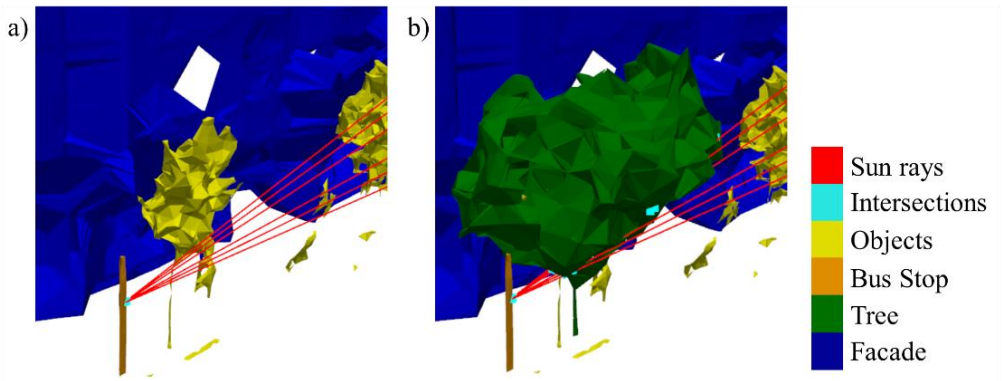

Figure 8. Sun rays from 15:15 to 16:45 in bus stop B: a) No intersections with small tree, b) Intersections with big tree

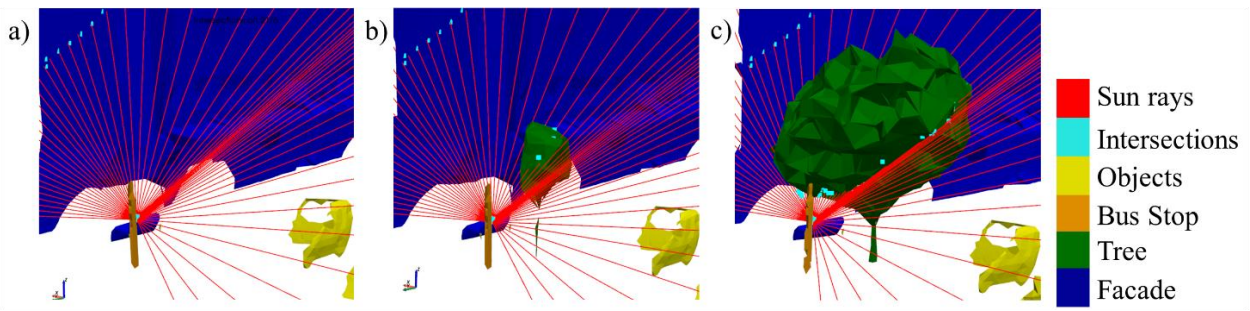

Figure 9. Intersections in bus stop C. a) Real bus stop, b) adding a small tree, c) adding a big tree

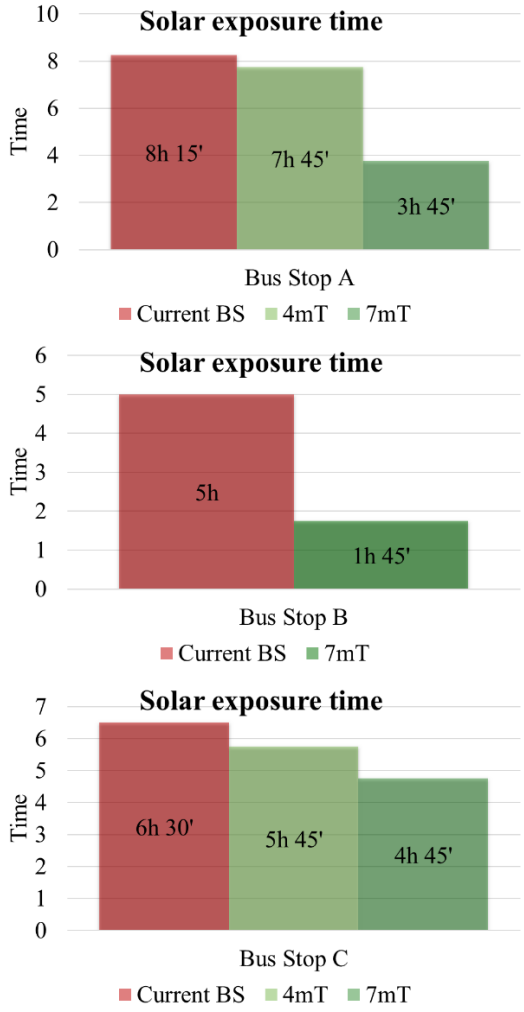

Figure 10. Solar exposure time. *BS (Bus Stop)

	BS A	BS B	BS C
4mT	30’	--	45’
7mT	4h 30’	3h 15’	1h 45’

Table 2. Solar exposure time reduction adding a 7mT and 4mT. *BS (Bus Stop)

3.3 Subsoil investigation with GPR

The GPR survey was conducted with a ProEx system using a ground-coupled antennas of 1.2 GHz and 500 MHz central frequencies. The data acquisition parameters selected were 1.0 cm of trace-interval distance and a total time window of 32 ns (536 samples per trace) and 78 ns (864 samples per trace), respectively. A total of 6 parallel profile lines were registered with both frequency antennas. To measure the profile length and to control the trace-interval distance, the antennas were mounted in a survey cart with an odometer wheel.

Before interpretation, the GPR signals received were processed with the software ReflexW to improve the imaging by using the following processing sequence: time-zero correction, subtract-mean (dewow), gain function, background removal and bandpass Butterworth.
Figure 11 shows the results obtained from profile line 1 (P1). Observing the radargram produced, it was possible to interpret the presence of manholes in the form of signal reverberation (red boxes), perpendicular pipes in the form of hyperbolic reflections (yellow/green ellipses/lines) and longitudinal pipes in the form of continuous flat reflections (dotted orange lines). Figure 12 presents the radargrams produced by profile line 3 (P3), showing the interpretation of perpendicular pipes. Finally, Figure 13 includes the radargrams obtained for profile lines 4, 5 and 6, also displaying the identification of perpendicular pipes. Additionally, this Figure 13 includes a complete illustration of the location of the objects interpreted.

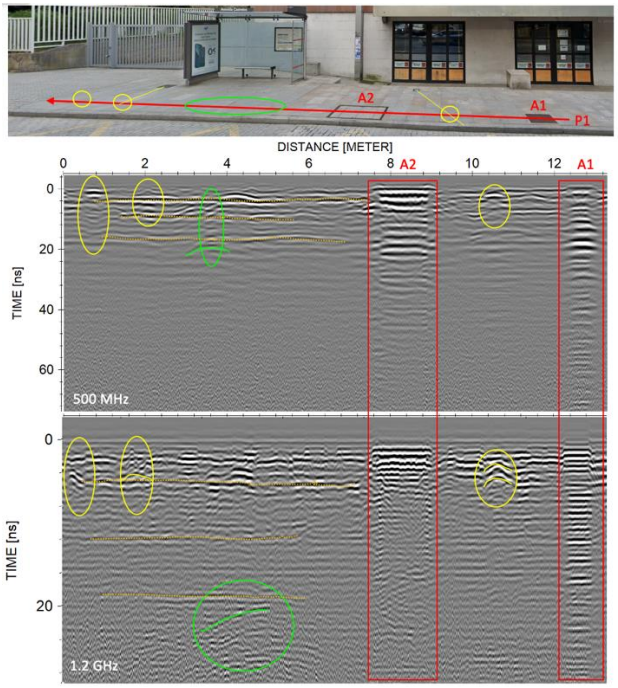

Figure 11. 500 MHz and 1.2 GHz radargrams obtained for P1, showing the interpretation of metallic manholes (highlighted into red boxes), perpendicular pipes (highlighted into yellow and green ellipses/lines), and longitudinal pipes (marked as dotted orange lines)

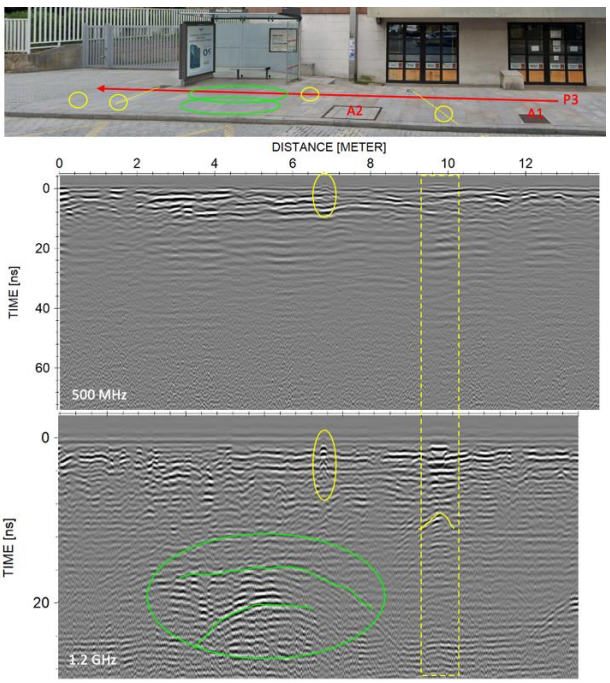

Figure 12. 500 MHz and 1.2 GHz radargrams obtained for P3, showing the interpretation of perpendicular pipes (highlighted into yellow and green ellipses/lines).

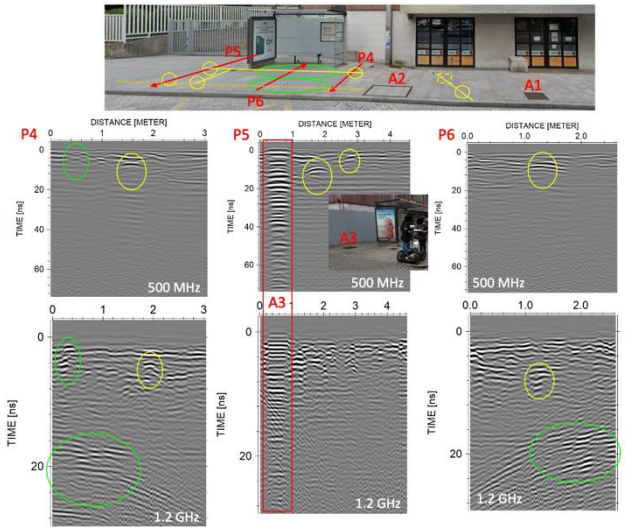

Figure 13. 500 MHz and 1.2 GHz radargrams obtained for P4, P5 and P6, showing the interpretation of a metallic manhole (highlighted into a red box) and perpendicular pipes (highlighted into yellow and green ellipses/lines).

4. Discussion

MLS allows for rapid data collection as it captures detailed 3D information of surroundings. With this technology it is possible to scan the urban environment and, therefore, bus stops. Nonetheless, certain limitations may arise due to potential occlusions. Additionally, ensuring the currency of point clouds is essential, especially considering that bus stop structures are subject to change. Results of solar exposure study possess that trees will occlude the sun glare. The tree height is significant as it extends the duration of sun occlusion, lasting longer at 7mT compared to 4mT. When assessing the selected tree, various factors can be considered, including its price, species, resistance to illness, and growth potential. These aspects play a pivotal role in ensuring the tree's suitability for the intended purpose and long-term viability within its environment.

While planting trees around bus stops proves to be an effective solution for mitigating sun glare, it is not always feasible to implement this solution, which depends on the ground. Urban areas often have underground pipes, which can hinder the planting of trees near a bus stop. GPR technology allows subsurface exploration without causing damage to the area being scanned, however the data acquisition with this technology is slower compared to MLS data acquisition. Conducting a GPR survey allows to examine subsurface elements and assists in identifying areas suitable for tree planting.

5. Conclusions

Urban transport is essential for the mobility of citizens and therefore thermal comfort at bus stops must be ensured. With the proposed method direct sun glare in bus stops are detected and reduced. The bus stop is located within the MLS point cloud, and its points are classified automatically into street objects, facades, and vertical bus stops. Subsequently, sun rays are calculated based on the sun angles. Results show that intersections of sun rays with the objects can be calculated with the proposed method.

The GPR survey enables an analysis of the ground beneath the bus stop's location, assessing the presence of underground pipes and determining the feasibility of integrating a tree within the vicinity of the bus stop. While this technology offers significant advantages, one of its limitations lies in manual interpretation. However, some pipes and metallic manholes were founded in the manual analysis.

The results indicate significant reductions in sun exposure hours at different bus stops. At bus stop A, introducing a 4mT resulted in a 6.1% reduction, while a 7mT led to a substantial 54.5% decrease. At bus stop B, a 4mT led to a 65% reduction in sun exposure hours. At bus stop C, implementing a 4mT resulted in an 11.5% decrease, while a 7mT showed a reduction of 26.9%. These findings affirm that the introduction of trees effectively diminishes sun exposure for users across various bus stops. Moreover, the incorporation of trees for shade brings about several additional benefits, including increased humidity, noise reduction, and a more relaxing environment compared to alternative artificial elements.

As future work, a study on solar occlusion in bus stops will be conducted using different tree species. Additionally, the growth time for each species will analyze to determine how long the tree will provide shade and block the solar glare.

Acknowledgments

The MLS work was funded by Government of Spain through project PDC2021-121239-C32 funded by MCIN/AEI/ 10.13039/501100011033 and RYC2022-038100-I funded by MCIN/AEI/10.13039/ 501100011033 and FSE+. The GPR work was funded by the Xunta de Galicia through the ENDITí project (ED431F 2021/08). M. Solla acknowledges the grant RYC2019–026604–I funded by MCIN/AEI/10.13039/501100011033 and by "ESF Investing in your future".

References

Balado, J., González, E., Arias, P., & Castro, D. (2020). Novel Approach to Automatic Traffic Sign Inventory Based on Mobile Mapping System Data and Deep Learning. *Remote Sensing*, *12*(3). https://doi.org/10.3390/rs12030442

Ballester, J., Quijal-Zamorano, M., Méndez Turrubiates, R. F., Pegenaute, F., Herrmann, F. R., Robine, J. M., Basagaña, X., Tonne, C., Antó, J. M., & Achebak, H. (2023). Heat-related mortality in Europe during the summer of 2022. *Nature Medicine*, *29*(7), 1857–1866. https://doi.org/10.1038/s41591-023-02419-z

Cabo, C., Ordoñez, C., García-Cortés, S., & Martínez, J. (2014). An algorithm for automatic detection of pole-like street furniture objects from Mobile Laser Scanner point clouds. *ISPRS Journal of Photogrammetry and Remote Sensing*, *87*, 47–56. https://doi.org/10.1016/j.isprsjprs.2013.10.008

Coutts, A. M., White, E. C., Tapper, N. J., Beringer, J., & Livesley, S. J. (2016). Temperature and human thermal comfort effects of street trees across three contrasting street canyon environments. *Theoretical and Applied Climatology*, *124*(1), 55–68. https://doi.org/10.1007/s00704-015-1409-y

Ebi, K. L., Capon, A., Berry, P., Broderick, C., Dear, R. de, Havenith, G., Honda, Y., Kovats, R. S., Ma, W., Malik, A., Morris, N. B., Nybo, L., Seneviratne, S. I., Vanos, J., & Jay, O. (2021). Hot weather and heat extremes: Health risks. *The Lancet*, *398*(10301), 698–708. https://doi.org/10.1016/S0140-6736(21)01208-3

González-Collazo, S. M., Balado, J., González, E., Lorenzo, H., & Díaz-Vilariño, L. (2022). DEFINING THE FUNCTIONAL SPACE OF BUS STOPS FROM MLS POINT CLOUDS. *ISPRS Annals of the Photogrammetry, Remote Sensing and Spatial Information Sciences*, *X-4/W2-2022*, 77–82. https://doi.org/10.5194/isprs-annals-X-4-W2-2022-77-2022

Ibeas, Á., dell'Olio, L., Alonso, B., & Sainz, O. (2010). Optimizing bus stop spacing in urban areas. *Transportation Research Part E: Logistics and Transportation Review*, *46*(3), 446–458. https://doi.org/10.1016/j.tre.2009.11.001

Jamei, E., Rajagopalan, P., Seyedmahmoudian, M., & Jamei, Y. (2016). Review on the impact of urban geometry and pedestrian level greening on outdoor thermal comfort. *Renewable and Sustainable Energy Reviews*, *54*, 1002–1017. https://doi.org/10.1016/j.rser.2015.10.104

Kong, L., Lau, K. K.-L., Yuan, C., Chen, Y., Xu, Y., Ren, C., & Ng, E. (2017). Regulation of outdoor thermal comfort by trees in Hong Kong. *Sustainable Cities and Society*, *31*, 12–25. https://doi.org/10.1016/j.scs.2017.01.018

Lombardi, F., Podd, F., & Solla, M. (2022). From Its Core to the Niche: Insights from GPR Applications. *Remote Sensing*, *14*(13). https://doi.org/10.3390/rs14133033

Melnikov, V. R., Christopoulos, G. I., Krzhizhanovskaya, V. V., Lees, M. H., & Sloot, P. M. A. (2022). Behavioural thermal regulation explains pedestrian path choices in hot urban environments. *Scientific Reports*, *12*(1), 2441. https://doi.org/10.1038/s41598-022-06383-5

Nasrollahi, N., Ghosouri, A., Khodakarami, J., & Taleghani, M. (2020). Heat-Mitigation Strategies to Improve Pedestrian Thermal Comfort in Urban Environments: A Review. *Sustainability*, *12*(23). https://doi.org/10.3390/su122310000

Ordóñez, C., Cabo, C., & Sanz-Ablanedo, E. (2017). Automatic Detection and Classification of Pole-Like Objects for Urban Cartography Using Mobile Laser Scanning Data. *Sensors*, *17*(7). https://doi.org/10.3390/s17071465

Ruiz, M. A., Sosa, M. B., Correa, E. N., & Cantón, M. A. (2017). Design tool to improve daytime thermal comfort and nighttime cooling of urban canyons. *Landscape and Urban Planning*, *167*, 249–256. https://doi.org/10.1016/j.landurbplan.2017.07.002

Schittekat, P., Kinable, J., Sörensen, K., Sevaux, M., Spieksma, F., & Springael, J. (2013). A metaheuristic for the school bus routing problem with bus stop selection. *European Journal of Operational Research*, *229*(2), 518–528. https://doi.org/10.1016/j.ejor.2013.02.025

Soilán, M., Riveiro, B., Martínez-Sánchez, J., & Arias, P. (2016). Traffic sign detection in MLS acquired point clouds for geometric and image-based semantic inventory. *ISPRS Journal of Photogrammetry and Remote Sensing*, *114*, 92–101. https://doi.org/10.1016/j.isprsjprs.2016.01.019

Solla, M., Pérez-Gracia, V., & Fontul, S. (2021). A Review of GPR Application on Transport Infrastructures: Troubleshooting and Best Practices. *Remote Sensing*, *13*(4). https://doi.org/10.3390/rs13040672

Speak, A. F., & Salbitano, F. (2022). Summer thermal comfort of pedestrians in diverse urban settings: A mobile study. *Building and Environment*, *208*, 108600. https://doi.org/10.1016/j.buildenv.2021.108600

Tan, Z., Lau, K. K.-L., & Ng, E. (2017). Planning strategies for roadside tree planting and outdoor comfort enhancement in subtropical high-density urban areas. *Building and Environment*, *120*, 93–109. https://doi.org/10.1016/j.buildenv.2017.05.017

Teo, T.-A., & Chiu, C.-M. (2015). Pole-Like Road Object Detection From Mobile Lidar System Using a Coarse-to-Fine Approach. *IEEE Journal of Selected Topics in Applied Earth Observations and Remote Sensing*, *8*, 1–14. https://doi.org/10.1109/JSTARS.2015.2467160

Tong, S., Wong, N. H., Tan, C. L., Jusuf, S. K., Ignatius, M., & Tan, E. (2017). Impact of urban morphology on microclimate and thermal comfort in northern China. *Solar Energy*, *155*, 212–223. https://doi.org/10.1016/j.solener.2017.06.027

Vailshery, L. S., Jaganmohan, M., & Nagendra, H. (2013). Effect of street trees on microclimate and air pollution in a tropical city. *Urban Forestry & Urban Greening*, *12*(3), 408–415. https://doi.org/10.1016/j.ufug.2013.03.002

Wang, C., Ji, M., Wang, J., Wen, W., Li, T., & Sun, Y. (2019). An Improved DBSCAN Method for LiDAR Data Segmentation with Automatic Eps Estimation. *Sensors*, *19*(1). https://doi.org/10.3390/s19010172

Wu, B., Yu, B., Yue, W., Shu, S., Tan, W., Hu, C., Huang, Y., Wu, J., & Liu, H. (2013). A Voxel-Based Method for Automated Identification and Morphological Parameters Estimation of Individual Street Trees from Mobile Laser Scanning Data. *Remote Sensing*, *5*(2), 584–611. https://doi.org/10.3390/rs5020584

Yan, W. Y., Morsy, S., Shaker, A., & Tulloch, M. (2016). Automatic extraction of highway light poles and towers from mobile LiDAR data. *Optics & Laser Technology*, *77*, 162–168. https://doi.org/10.1016/j.optlastec.2015.09.017

Yu, B., Lam, W. H. K., & Tam, M. L. (2011). Bus arrival time prediction at bus stop with multiple routes. *Transportation Research Part C: Emerging Technologies*, *19*(6), 1157–1170. https://doi.org/10.1016/j.trc.2011.01.003

Yu, Y., Li, J., Guan, H., Wang, C., & Yu, J. (2015). Semiautomated Extraction of Street Light Poles From Mobile LiDAR Point-Clouds. *Geoscience and Remote Sensing, IEEE Transactions On*, *53*, 1374–1386. https://doi.org/10.1109/TGRS.2014.2338915